ELSEVIER

Comput. Methods Appl. Mech. Engrg. 166 (1998) 3–24

Computer methods in applied mechanics and engineering

The variational multiscale method—a paradigm for computational mechanics

Thomas J.R. Hughes*, Gonzalo R. Feijóo[1], Luca Mazzei[1], Jean-Baptiste Quincy[1]

Division of Mechanics and Computation, Durand Building, Stanford University, Stanford, CA 94305, USA

Received 28 January 1998; revised 11 February 1998

Abstract

We present a general treatment of the variational multiscale method in the context of an abstract Dirichlet problem. We show how the exact theory represents a paradigm for subgrid-scale models and a posteriori error estimation. We examine hierarchical p-methods and bubbles in order to understand and, ultimately, approximate the 'fine-scale Green's function' which appears in the theory. We review relationships between residual-free bubbles, element Green's functions and stabilized methods. These suggest the applicability of the methodology to physically interesting problems in fluid mechanics, acoustics and electromagnetics.

1. Introduction

The variational multiscale method was introduced in [10] and [13] as a procedure for deriving models and numerical methods capable of dealing with multiscale phenomena ubiquitous in science and engineering. It is motivated by the simple fact that straightforward application of Galerkin's method employing standard bases, such as Fourier series and finite elements, is *not* a robust approach in the presence of multiscale phenomena. The variational multiscale method seeks to rectify this situation. The anatomy of the method is simple: we look at *sum decompositions* of the solution, $u = \bar{u} + u'$, where we think of solving for $\bar{u}$ *numerically*, but we attempt to determine u' *analytically*, eliminating it from the problem for $\bar{u}$. $\bar{u}$ and u' may *overlap* or be *disjoint*, and u' may be *globally* or *locally* defined (see [10] for examples). The effect of u' on the problem for $\bar{u}$ will always be *nonlocal*. In this paper we will confine our attention to cases in which $\bar{u}$ represents 'coarse scales' and u' 'fine scales'.

We attempt to present the 'big picture' in the context of an abstract Dirichlet problem involving a second-order differential operator which we permit to be nonsymmetric and/or indefinite. This allows us to consider equations of practical interest, such as the advection–diffusion equation, a model for fluid mechanics phenomena, and the Helmholtz equation, of importance in acoustics and electromagnetics. After introducing the variational formulation of the Dirichlet problem, we consider its multiscale version.

First, we consider the 'smooth case', in which we assume that all functions are sufficiently smooth so that distributional effects (e.g. Dirac layers) may be ignored. This enables a simple derivation of the exact equation governing the coarse scales. It is helpful to think of this case as pertaining to the situation in which both the coarse and fine scales are represented by Fourier series.

* Corresponding author. Professor of Mechanical Engineering. Chairman of the Division of Mechanics and Computation.

[1] Graduate Research Assistant.

0045-7825/98/$19.00
PII: S0045-7825(98)00079-6

We next consider a case of greater practical interest in which standard finite elements are employed to represent the coarse scales. Due to lack of continuity of derivatives at element interfaces, we need to explicitly account for the distributional effects omitted in the smooth case. We refer to this as the 'rough case'. Again, we derive an exact equation governing the behavior of coarse scales. It is this equation that we propose as a paradigm for developing subgrid-scale models. Two distinguishing features characterize this result. The first is that the method may be viewed as the classical Galerkin method plus an additional term driven by the *distributional* residual of the coarse scales. This involves residuals of the partial differential equation under consideration on element interiors (this is the smooth part of the residual), and jump terms involving the boundary operator on element interfaces (this is the rough part deriving from Dirac layers in the distributional form of the operator). The appearance of element residuals and jump terms are suggestive of the relationship between the multiscale formulation and various *stabilized methods* proposed previously. The second distinguishing feature is the appearance of the fine-scale Green's function. In general, this is *not* the classical Green's function, but one that emanates from the fine-scale subspace. It is important to note that the fine-scale subspace, $\mathcal{V}'$, is infinite-dimensional, but a proper subspace of the space, $\mathcal{V}$, in which we attempt to solve the problem. We have the direct sum relationship $\mathcal{V}=\overline{\mathcal{V}}\oplus\mathcal{V}'$ where $\overline{\mathcal{V}}$ is the coarse-scale, finite element subspace. The problem that we are faced with in developing practical approximations is that the fine-scale Green's function is *nonlocal*.

Before addressing this issue, we discuss the relationship between the fine-scale solution and a posteriori error estimation. We first note that by virtue of the formulation being exact, the fine-scale solution is precisely the error in the coarse-scale solution. Consequently, the representation obtained of the fine-scale solution in terms of the distributional coarse-scale residual and the fine-scale Green's function is a paradigm for a posteriori error estimation. We note that it is typical in proposed a posteriori error estimation procedures to involve the element residuals and/or interface jump terms as driving mechanisms. The mode of distributing these sources of error may thus be inferred to be approximations of the fine-scale Green's function. As a result, it is clear that in a posteriori error estimation, the proper distribution of residual errors strongly depends on the operator under consideration. In other words, there is no universally appropriate scheme independent of the operator. (A similar observation may be made for subgrid-scale models by virtue of the form of the coarse-scale equation.) We discuss the implications of the formula for the fine-scale solution with respect to a posteriori error estimation for finite element approximations of the advection–diffusion and Helmholtz equations.

We next examine hierarchical p-refinement and bubbles in an effort to better understand the nature of the fine-scale Green's function and to deduce appropriate forms. We identify $\overline{\mathcal{V}}$ with standard, low-order finite elements, and $\mathcal{V}'$ with the hierarchical basis. We derive an explicit formula for the fine-scale Green's function in terms of the hierarchical basis. We conclude that, despite the nonlocal character of the fine-scale Green's function, it can always be represented in terms of a finite basis of functions possessing local support. In one dimension, this basis consists solely of bubbles, in two dimensions, bubbles and edge functions; etc. This reduces the problem of approximating the Green's function to one of obtaining a good-quality, finite-dimensional fine-scale basis. This becomes the fundamental problem in the construction of practical methods. Once solved, we have a subgrid-scale model governing the coarse-scales, *and* an approximate representation of the fine-scale solution which does double duty as an a posteriori error estimator for the coarse-scale solution.

We begin the discussion of what constitutes a good-quality, but practical, fine-scale basis by reviewing the concept of residual-free bubbles (see [1]). We then review the use of fine-scale Green's functions supported by individual elements. Residual-free bubbles and element Green's functions are intimately related as shown in Brezzi et al. [2]. We then review how these concepts may be used to derive stabilized methods and identify optimal parameters which appear in their definition. We illustrate these ideas with one-dimensional examples.

Despite the success of the residual-free concept, there is still need for improvement. As evidence of this fact, we note that solutions of the advection–diffusion equation with sharp internal and boundary layers give rise to spurious localized oscillations for stabilized methods which are effectively identical to residual-free bubble methods. Thus, we explore the possibilities of even higher-fidelity methods by expanding the residual-free basis to include edge functions in two dimensions, etc. This poses significant analytical complexity, but we speculate on some preliminary ideas of approximation which may be both practical and beneficial.

We conclude with a summary of results and identification of some outstanding issues.

The overall flow of the main relationships is presented in Fig. 1.

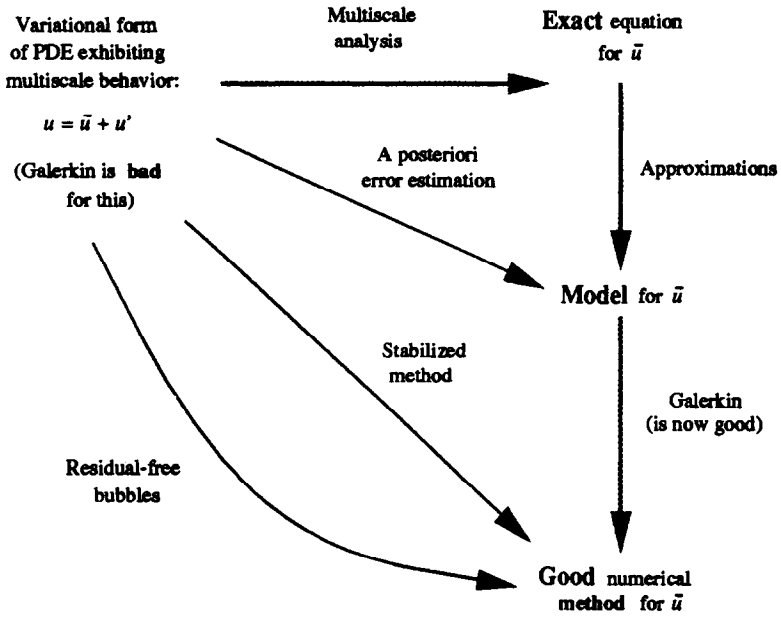

Fig. 1. The variational multiscale method is a framework for the construction of subgrid-scale models and effective numerical methods for partial differential equations exhibiting multiscale phenomena. It provides a physical context for understanding methods based on residual-free bubbles and stabilized methods.

2. Abstract Dirichlet problem

Let $\Omega \subset \mathbb{R}^d$, where $d \geq 1$ is the number of space dimensions, be an open, bounded domain with smooth boundary Γ (see Fig. 2). We consider the following boundary-value problem:

Find $u : \Omega \to \mathbb{R}$ such that

$$\mathscr{L}u = f \quad \text{in } \Omega \tag{1}$$

$$u = g \quad \text{on } \Gamma \tag{2}$$

where $f : \Omega \to \mathbb{R}$ and $g : \Gamma \to \mathbb{R}$ are given functions. We wish to think of $\mathscr{L}$ as a second-order and, in general, *nonsymmetric* differential operator.

2.1. Variational formulation

Let $\mathscr{S} \subset H^1(\Omega)$ denote the *trial solution space* and $\mathscr{V} \subset H^1(\Omega)$ denote the *weighting function space*, where $H^1(\Omega)$ is the Sobolev space of square-integrable functions with square-integrable derivatives. We assume that $\mathscr{S}$

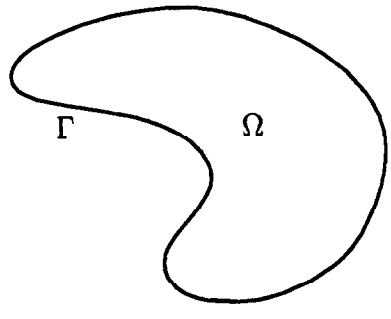

Fig. 2. Domain and boundary for the abstract Dirichlet problem.

and $\mathcal{V}$ possess the following properties

$$u = g \quad \text{on } \Gamma \quad \forall\, u \in \mathcal{S} \tag{3}$$

$$w = 0 \quad \text{on } \Gamma \quad \forall\, w \in \mathcal{V} \tag{4}$$

The variational counterpart of the boundary-value problem (1)–(2) is given as follows:
Find $u \in \mathcal{S}$ such that $\forall\, w \in \mathcal{V}$

$$a(w, u) = (w, f) \tag{5}$$

where $(\cdot, \cdot)$ is the $L_2(\Omega)$ inner product, and $a(\cdot, \cdot)$ is a bilinear form satisfying

$$a(w, u) = (w, \mathcal{L}u) \tag{6}$$

for all *sufficiently smooth* $w \in \mathcal{V}$ and $u \in \mathcal{S}$.

3. Variational multiscale method

Let

$$u = \bar{u} + u' \quad (\textit{overlapping} \text{ sum decomposition}) \tag{7}$$

where $\bar{u}$ represents *coarse scales* and u' represents *fine scales* (see Fig. 3). Likewise, let

$$w = \bar{w} + w' . \tag{8}$$

Let $\mathcal{S} = \bar{\mathcal{S}} \oplus \mathcal{S}'$ and $\mathcal{V} = \bar{\mathcal{V}} \oplus \mathcal{V}'$ where $\bar{\mathcal{S}}$ (resp. $\mathcal{S}'$) is the trial solution space for *coarse* (resp. *fine*) scales and $\bar{\mathcal{V}}$ (*resp.* $\mathcal{V}'$) is the weighting function space for *coarse* (resp. *fine*) scales. We assume

$$\bar{u} = g \quad \text{on } \Gamma \quad \forall\, \bar{u} \in \bar{\mathcal{S}} \tag{9}$$

$$u' = 0 \quad \text{on } \Gamma \quad \forall\, u' \in \mathcal{S}' \tag{10}$$

$$\bar{w} = 0 \quad \text{on } \Gamma \quad \forall\, \bar{w} \in \bar{\mathcal{V}} \tag{11}$$

$$w' = 0 \quad \text{on } \Gamma \quad \forall\, w' \in \mathcal{V}' \tag{12}$$

Our objective is to derive an equation governing $\bar{u}$.

REMARK. It is helpful to think of $\bar{\mathcal{S}}$ and $\bar{\mathcal{V}}$ as finite-dimensional, whereas $\mathcal{S}'$ and $\mathcal{V}'$ are necessarily infinite-dimensional.

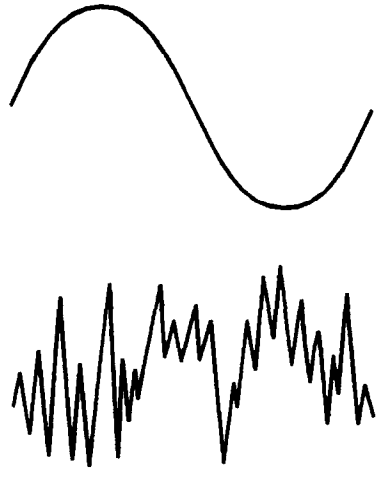

Fig. 3. Coarse and fine scale components.

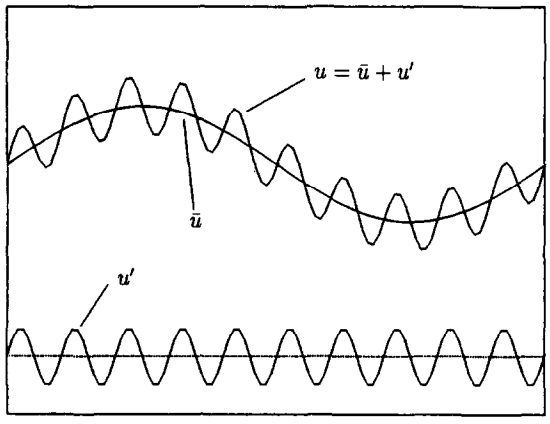

Fig. 4. The case in which $\bar{u}$ and u' are smooth.

3.1. Smooth case

We begin the developments by considering the case in which all functions are smooth. The idea for $u = \bar{u} + u'$ is illustrated in Fig. 4. The situation for $w = \bar{w} + w'$ is similar. We assume the following integration-by-parts formulas hold:

$$a(\bar{w}, u') = (\mathscr{L}^*\bar{w}, u') \quad \forall\, \bar{w} \in \bar{\mathscr{V}},\ u' \in \mathscr{S}' \tag{13}$$

$$a(w', \bar{u}) = (w', \mathscr{L}\bar{u}) \quad \forall\, w' \in \mathscr{V}',\ \bar{u} \in \bar{\mathscr{S}} \tag{14}$$

$$a(w', u') = (w', \mathscr{L}u') \quad \forall\, w' \in \mathscr{V}',\ u' \in \mathscr{S}' \tag{15}$$

3.1.1. Exact variational equation for $\bar{u}$ (smooth case)

We substitute (7) and (8) into (5):

$$a(\bar{w} + w', \bar{u} + u') = (\bar{w} + w', f) \quad \forall\, \bar{w} \in \bar{\mathscr{V}},\quad \forall\, w' \in \mathscr{V}' \tag{16}$$

By virtue of the linear independence of $\bar{w}$ and w', (16) splits into two problems:

Problem (1)

$$a(\bar{w}, \bar{u}) + a(\bar{w}, u') = (\bar{w}, f) \quad \forall\, \bar{w} \in \bar{\mathscr{V}} \tag{17}$$

$$a(\bar{w}, \bar{u}) + (\mathscr{L}^*\bar{w}, u') = (\bar{w}, f) \tag{18}$$

Problem (2)

$$a(w', \bar{u}) + a(w', u') = (w', f) \quad \forall\, w' \in \mathscr{V}' \tag{19}$$

$$(w', \mathscr{L}\bar{u}) + (w', \mathscr{L}u') = (w', f) \tag{20}$$

In arriving at (18) and (20), we have employed the integration-by-parts formulas (13)–(15). We may rewrite (20) as

$$\Pi' \mathscr{L}u' = -\Pi'(\mathscr{L}\bar{u} - f) \quad \text{in } \Omega \tag{21}$$

$$u' = 0 \quad \text{on } \Gamma \tag{22}$$

where Π' is the L_2-projection onto $\mathscr{V}'$. We endeavor to solve this problem for u' and eliminate u' from the equation for $\bar{u}$, namely (18). This can be accomplished with the aid of a Green's function.

3.1.2. Green's function for the 'dual problem'

Consider the following Green's function problem for the adjoint operator:

$$\Pi' \mathscr{L}^* g'(x, y) = \Pi' \delta(x - y) \quad \forall\, x \in \Omega \tag{23}$$

$$g'(x, y) = 0 \quad \forall\, x \in \Gamma \tag{24}$$

In terms of the solution of this problem, u' can be expressed as follows:

$$u'(y) = -\int_{\Omega} g'(x, y)(\mathscr{L}\bar{u} - f)(x)\, d\Omega_x \tag{25}$$

Equivalently, we can write (25) in terms of an integral operator M' as

$$u' = M'(\mathscr{L}\bar{u} - f) \tag{26}$$

REMARKS

(1) $\mathscr{L}\bar{u} - f$ is the *residual* of the coarse scales.
(2) The fine scales u' are *driven* by the residual of the coarse scales.
(3) It is very important to observe that g' is *not* the usual Green's function associated with the corresponding strong form of (23). Rather, g' is defined entirely in terms of the space of fine scales, namely $\mathscr{V}'$. Later on we will derive an explicit formula for g' in terms of a basis for $\mathscr{V}'$.

Substituting (26) into (18) yields

$$\boxed{a(\bar{w}, \bar{u}) + (\mathscr{L}^*\bar{w}, M'(\mathscr{L}\bar{u} - f)) = (\bar{w}, f) \quad \forall\, \bar{w} \in \bar{\mathscr{V}}} \tag{27}$$

where, from (25),

$$(\mathscr{L}^*\bar{w}, M'(\mathscr{L}\bar{u} - f)) = -\int_{\Omega}\int_{\Omega} (\mathscr{L}^*\bar{w}(y)g'(x, y)(\mathscr{L}\bar{u} - f)(x)\, d\Omega_x\, d\Omega_y \tag{28}$$

REMARKS

(1) This is an *exact* equation for the coarse scales.
(2) The effect of the fine scales on the coarse scales is *nonlocal.*
(3) By virtue of the smoothness assumptions, this result is appropriate for spectral methods, or methods based on Fourier series, but it is not sufficiently general as a basis for finite-element methods. In what follows, we relax the smoothness assumption and consider the form of the coarse scale equation appropriate for finite elements.

3.2. Rough case (FEM)

We consider a discretization of Ω into finite elements. The domain and boundary of element e, where $e \in \{1, 2, \ldots, n_{el}\}$, in which n_{el} is the number of elements, are denoted Ω^e and Γ^e, respectively (see Fig. 5). The union of element interiors is denoted Ω' and the union of element boundaries modulo Γ (also referred to as the *element interfaces*) is denoted Γ', viz.

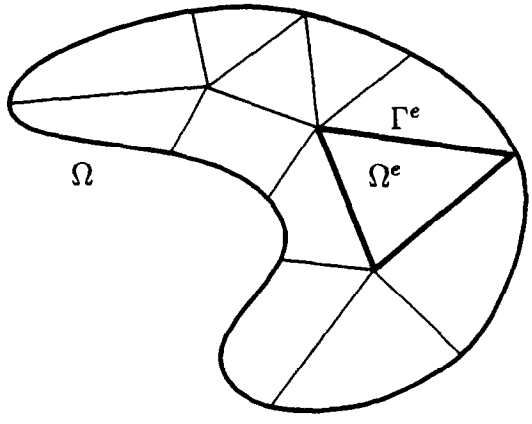

Fig. 5. Discretization of Ω into element subdomains.

$$\Omega' = \bigcup_{e=1}^{n_{el}} \Omega^e \tag{29}$$

$$\Gamma' = \left(\bigcup_{e=1}^{n_{el}} \Gamma^e \right) \Gamma \tag{30}$$

$$\overline{\Omega} = \text{closure}(\Omega') \tag{31}$$

Let $\overline{\mathscr{S}}, \overline{\mathscr{V}} \subset C^0(\overline{\Omega}) \cap H^1(\Omega)$ be classical finite element spaces. Note $\mathscr{S}', \mathscr{V}' \subset H^1(\Omega)$, but are otherwise arbitrary. In this case $\overline{u}$ and $\overline{w}$ are smooth on element interiors but have slope discontinuities across element boundaries (see e.g. Fig. 6).

We need to introduce some terminology used in the developments which follow. Let $(\cdot,\cdot)_\omega$ be the $L_2(\omega)$ inner product where $\omega = \Omega, \Omega^e, \Gamma^e, \Omega', \Gamma'$, etc. Recall, $(\cdot,\cdot) = (\cdot,\cdot)_\Omega$. Let $[\![\cdot]\!]$ denote the *jump operator*, viz. if $\boldsymbol{v}$ is a vector field experiencing a discontinuity across an element boundary (e.g. $\boldsymbol{v} = \nabla\overline{w}$, $\overline{w} \in \overline{\mathscr{V}}$), then

$$\begin{aligned} [\![\boldsymbol{n}\cdot\boldsymbol{v}]\!] &= \boldsymbol{n}^+\cdot\boldsymbol{v}^+ + \boldsymbol{n}^-\cdot\boldsymbol{v}^- \\ &= \boldsymbol{n}^+\cdot\boldsymbol{v}^+ - \boldsymbol{n}^+\cdot\boldsymbol{v}^- \\ &= \boldsymbol{n}\cdot(\boldsymbol{v}^+ - \boldsymbol{v}^-), \end{aligned} \tag{32}$$

where

$$\boldsymbol{n} = \boldsymbol{n}^+ = -\boldsymbol{n}^- \tag{33}$$

is a unit normal vector on the element boundary and the $\pm$ designations are defined as illustrated in Fig. 7. Note that (32) is invariant with respect to interchange of $\pm$ designations.

In the present case we only have smoothness on element interiors. Consequently, integration-by-parts gives rise to nonvanishing element boundary terms. For example, if $\overline{w} \in \overline{\mathscr{V}}$ and $u' \in \mathscr{S}'$, the following integration-by-parts formula holds

$$\begin{aligned} a(\overline{w}, u') &= \sum_{e=1}^{n_{el}} ((\mathscr{L}^*\overline{w}, u')_{\Omega^e} + (b^*\overline{w}, u')_{\Gamma^e}) \\ &= (\mathscr{L}^*\overline{w}, u')_{\Omega'} + ([\![b^*\overline{w}]\!], u')_{\Gamma'} \\ &= (\mathscr{L}^*\overline{w}, u')_{\Omega} \end{aligned} \tag{34}$$

where b^* is the *boundary operator* corresponding to $\mathscr{L}^*$ (e.g. if $\mathscr{L}^* = \mathscr{L} = -\Delta$, then $b^* = b = \boldsymbol{n}\cdot\nabla = \partial/\partial n$). Note, from (34), there are three different ways to express the integration-by-parts formula. The first line of (34) amounts to performing integration-by-parts on an element-by-element basis. In the second line, the sum over element interiors has been represented by integration over Ω' and the element boundary terms have been

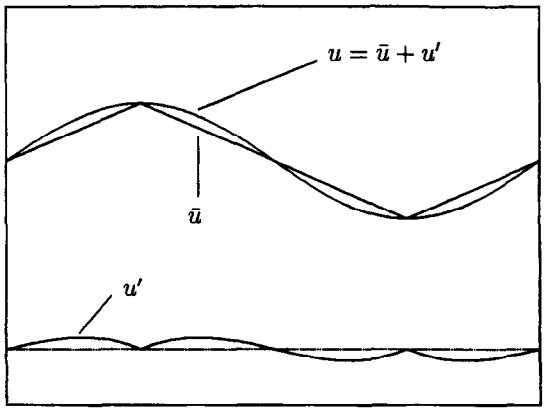

Fig. 6. $\overline{u}$ is the piecewise linear interpolate of u.

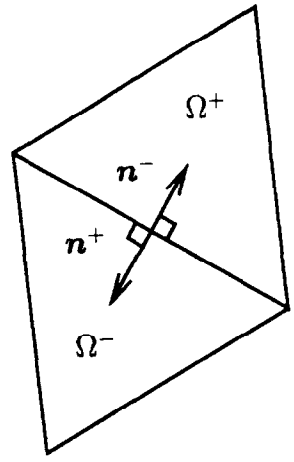

Fig. 7. Definition of unit normals on an element boundary.

combined in pairs, the result being a jump term integrated over element interfaces. Finally, in the third line, we view $\mathscr{L}^*\overline{w}$ as a *Dirac distribution* defined on the entire domain Ω. To understand this interpretation, consider the following example:

Let

$$\mathscr{L}^*\overline{w} = \overline{w}_{,xx} \tag{35}$$

and assume $\overline{w}$ consists of piecewise linear, or quadratic, finite elements in one dimension. The set-up is illustrated in Fig. 8. Note that $\overline{w}_{,xx}$ consists of Dirac delta functions at element boundaries and smooth functions on element interiors. This amounts to the distributional interpretation of $\mathscr{L}^*\overline{w}$ in the general case. It is smooth on element interiors but contains Dirac layers on the element interfaces, which give rise to the jump terms in the second line of (34).

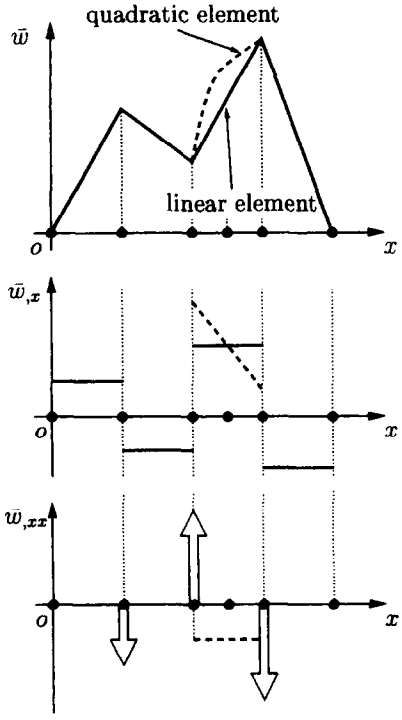

Fig. 8. Generalized derivatives of piecewise linear and quadratic finite elements.

Likewise, we have the additional integration-by-parts formulas: $\forall\, w' \in \mathcal{V}'$, $\bar{u} \in \bar{\mathcal{S}}$ and $u' \in \mathcal{S}'$,

$$\begin{aligned} a(w', \bar{u}) &= \sum_{e=1}^{n_{el}} ((w', \mathcal{L}\bar{u})_{\Omega^e} + (w', b\bar{u})_{\Gamma^e}) \\ &= (w', \mathcal{L}\bar{u})_{\Omega'} + (w', [\![b\bar{u}]\!])_{\Gamma'} \\ &= (w', \mathcal{L}\bar{u})_{\Omega} \end{aligned} \tag{36}$$

$$\begin{aligned} a(w', u') &= \sum_{e=1}^{n_{el}} ((w', \mathcal{L}u')_{\Omega^e} + (w', bu')_{\Gamma^e}) \\ &= (w', \mathcal{L}u')_{\Omega'} + (w', [\![bu']\!])_{\Gamma'} \\ &= (w', \mathcal{L}u')_{\Omega} \end{aligned} \tag{37}$$

where, again, $\mathcal{L}\bar{u}$ and $\mathcal{L}u'$ are *Dirac distributions* on Ω.

3.2.1. Exact variational equation for $\bar{u}$ (rough case)

The distributional interpretation of $\mathcal{L}\bar{u}$, $\mathcal{L}u'$ and $\mathcal{L}^*\bar{w}$ allows us to follow the developments of the smooth case (see Section 3.1.1). Thus, the formula for u' can be expressed in three alternative forms analogous to those of the integration-by-parts formulas, viz.

$$\begin{aligned} u'(y) &= -\int_{\Omega} g'(x, y)(\mathcal{L}\bar{u} - f)(x)\, d\Omega_x \\ &= -\int_{\Omega'} g'(x, y)(\mathcal{L}\bar{u} - f)(x)\, d\Omega_x - \int_{\Gamma'} g'(x, y)[\![b\bar{u}]\!](x)\, d\Gamma_x \\ &= -\sum_{e=1}^{n_{el}} \left(\int_{\Omega^e} g'(x, y)(\mathcal{L}\bar{u} - f)(x)\, d\Omega_x + \int_{\Gamma^e} g'(x, y)(b\bar{u})(x)\, d\Gamma_x \right) \end{aligned} \tag{38}$$

which we may again write succintly as $u' = M'(\mathcal{L}\bar{u} - f)$. Note, this is an *exact* formula for u'.

REMARKS

(1) When a mesh-based method, such as finite elements, is employed, the coarse scales, $\bar{u}$, are referred to as the *resolved scales*, and the fine scales, u', are referred to as the *subgrid scales*. The coarse-scale equation is often referred to as a *subgrid-scale model*.

(2) $\mathcal{L}\bar{u} - f$ is the *residual* of the resolved scales. It consists of a *smooth part* on element interiors (i.e., Ω') and a *jump term* $[\![b\bar{u}]\!]$ across element interfaces (i.e., Γ').

(3) The subgrid scales u' are *driven* by the residual of the resolved scales.

Upon substituting (38) into the equation for the coarse scales, we once again arrive at (27) where,

$$\begin{aligned} (\mathcal{L}^*\bar{w}, M'(\mathcal{L}\bar{u} - f)) &= -\int_{\Omega}\int_{\Omega} (\mathcal{L}^*\bar{w})(y) g'(x, y)(\mathcal{L}\bar{u} - f)(x)\, d\Omega_x\, d\Omega_y \\ &= -\int_{\Omega'}\int_{\Omega'} (\mathcal{L}^*\bar{w})(y) g'(x, y)(\mathcal{L}\bar{u} - f)(x)\, d\Omega_x\, d\Omega_y \\ &\quad -\int_{\Omega'}\int_{\Gamma'} (\mathcal{L}^*\bar{w})(y) g'(x, y)[\![b\bar{u}]\!](x)\, d\Gamma_x\, d\Omega_y \\ &\quad -\int_{\Gamma'}\int_{\Omega'} [\![b^*\bar{w}]\!](y) g'(x, y)(\mathcal{L}\bar{u} - f)(x)\, d\Omega_x\, d\Gamma_y \\ &\quad -\int_{\Gamma'}\int_{\Gamma'} [\![b^*\bar{w}]\!](y) g'(x, y)[\![b\bar{u}]\!](x)\, d\Gamma_x\, d\Gamma_y \\ &= -\sum_{e=1}^{n_{el}}\sum_{l=1}^{n_{el}} \left(\int_{\Omega^e}\int_{\Omega^l} (\mathcal{L}^*\bar{w})(y) g'(x, y)(\mathcal{L}\bar{u} - f)(x)\, d\Omega_x\, d\Omega_y \right. \end{aligned}$$

$$
\begin{aligned}
&- \int_{\Omega^e} \int_{\Gamma^I} (\mathscr{L}^* \overline{w})(y) g'(x, y)(b\overline{u})(x) \, d\Gamma_x \, d\Omega_y \\
&- \int_{\Gamma^e} \int_{\Omega^I} (b^* \overline{w})(y) g'(x, y)(\mathscr{L}\overline{u} - f)(x) \, d\Omega_x \, d\Gamma_y \\
&- \int_{\Gamma^e} \int_{\Gamma^I} (b^* \overline{w})(y) g'(x, y)(b\overline{u})(x) \, d\Gamma_x \, d\Gamma_y \Big)
\end{aligned} \tag{39}
$$

Note, once again, there are three alternative forms due to the distributional nature of $\mathscr{L}^*\overline{w}$ and $\mathscr{L}\overline{u}$.

REMARKS

(1) Eq. (27) along with (39) is an *exact* equation for the resolved scales. It can serve as a *paradigm* for finite element methods when unresolved scales are present.
(2) The effect of the unresolved scales on the resolved scales is *nonlocal.*
(3) The necessity of including jump operator terms to attain stable discretizations for certain problems has been observed previously by Hughes, Franca, Hulbert and others (see [4,9,11,12,14]). Franca and Russo [5] showed that jump terms arise naturally when residual-free macro-bubbles are eliminated. The present result is believed to be the first one in which the jump operator terms are *derived* directly from the governing equations for the fully general case.
(4) Eq. (39) illustrates that the distributional parts of $\mathscr{L}^*\overline{w}$ and $\mathscr{L}\overline{u}$ need to be included in a consistent stabilized method. Classically, these terms have been omitted, which has led to some problems. Jansen et al. [15] observed the need to include the effect of the distributional term. In their approach, rather than explicitly including the jump terms, a variational reconstruction of second-derivative terms is employed. Jansen et al. [15] showed that *significant* increases in accuracy are attained thereby. Leo Franca (private communication) observed the same phenomenon in another context. In joint work with Marek Behr and Tayfun Tezduyar, in which a three-field variational formulation was employed, no second derivatives appeared and consequently no distributional terms. As in the work of Jansen et al., increased accuracy was achieved.

We can write (27) concisely as

$$
\boxed{B(\overline{w}, \overline{u}; g') = L(\overline{w}; g') \quad \forall\, \overline{w} \in \overline{\mathscr{V}}} \tag{40}
$$

where

$$
B(\overline{w}, \overline{u}; g') = a(\overline{w}, \overline{u}) + (\mathscr{L}^*\overline{w}, M'(\mathscr{L}\overline{u})) \tag{41}
$$

$$
L(\overline{w}; g') = (\overline{w}, f) + (\mathscr{L}^*\overline{w}, M'f) \tag{42}
$$

Note that $B(\cdot, \cdot; \cdot)$ is bilinear with respect to the first two arguments and affine with respect to the third argument; $L(\cdot; \cdot)$ is linear with respect to the first argument and affine with respect to the second. Eqs. (40)–(42) are valid in both the smooth and rough cases, with the distributional interpretation appropriate in the latter case.

3.2.2. Numerical method

An *approximation*, $\tilde{g}' \approx g'$, is the key ingredient in developing a practical numerical method. It necessarily will entail some form of *localization*. We write the numerical method as follows:

$$
\boxed{B(\overline{w}^h, \overline{u}^h; \tilde{g}') = L(\overline{w}^h; \tilde{g}') \quad \forall\, \overline{w} \in \overline{\mathscr{V}}} \tag{43}
$$

3.2.3. u' and a posteriori error estimation

Note that $u' = u - \overline{u}$ is the *error* in the coarse scales. The formula $u' = M'(\mathscr{L}\overline{u}^h - f)$ is a *paradigm* for a posteriori error estimation. Thus, it is plausible that

$$u' \approx \tilde{M}'(\mathscr{L}\bar{u}^h - f) \tag{44}$$

where $\tilde{M}' \approx M'$, is an a posteriori *error estimator*, which can be used to estimate coarse-scale error in any suitable norm, e.g. the W_p^s-norm, $0 \leq p \leq \infty$, $0 \leq s < \infty$. (Keep in mind, $\mathscr{L}\bar{u}$ is a Dirac distribution.) An approximation of the fine-scale Green's function, $\tilde{g}' \approx g'$, induces an approximation $\tilde{M}' \approx M'$; see (38). Conversely, an a posteriori error estimator of the form (44) may be used to infer an approximation of the Green's function and to develop a numerical method of the form (43).

A particularly insightful form of the estimator is given by

$$\boxed{u'(y) \approx -\int_{\Omega'} \tilde{g}'(x, y)(\mathscr{L}\bar{u}^h - f)(x)\, d\Omega_x - \int_{\Gamma'} \tilde{g}'(x, y)[\![b\bar{u}^h]\!](x)\, d\Gamma_x} \tag{45}$$

Note that the residuals of the computed coarse-scale solution, that is $\mathscr{L}\bar{u}^h - f$ and $[\![b\bar{u}^h]\!]$, are the *sources* of error and the fine-scale Green's function acts as the *distributor* of error.

There seems to be agreement in the literature on a posteriori estimators that either one of, or both, the residuals are the sources of error. Where there seems to be considerable disagreement is in how the sources are distributed. From (45), we see that there is no universal solution to the question of what constitutes an appropriate distribution scheme. It is strongly dependent on the particular operator $\mathscr{L}$ through the fine-scale Green's function. This result may serve as a context for understanding differences of opinion which have occurred over procedures of a posteriori error estimation.

REMARK. An advantage of the variational multiscale method is that it comes *equipped* with a fine-scale solution which may be viewed as an a posteriori estimate of the coarse-scale solution error.

DISCUSSION. Let us examine the behavior of the exact counterpart of (45) for different operators of interest. Assume that u^h is piecewise linear in all cases, and that $f = 0$.

First, consider the Laplace operator, $\mathscr{L} = -\Delta$, $b = \partial/\partial n$. In this case, $\mathscr{L}\bar{u}^h = 0$, and the interface residual, $[\![b\bar{u}^h]\!]$, is the entire source of error. Keeping in mind the highly local nature of the Green's function for the Laplacian, a local distribution of $[\![b\bar{u}^h]\!]$ would seem to be a reasonable approximation. The same could be said for linear elasticity, assuming there are no constraints, such as, for example, incompressibility, or unidirectional inextensibility.

Next, consider the advection–diffusion operator, $\mathscr{L} = \boldsymbol{a} \cdot \nabla - \kappa\Delta$, $[\![b\bar{u}^h]\!] = [\![\kappa\, \partial\bar{u}^h/\partial n]\!]$[1], where $\boldsymbol{a}$ is a given solenoidal velocity field, and $\kappa > 0$, the diffusivity, is a positive constant. In the case of diffusion domination (i.e. advective effects are negligible), $\mathscr{L} \approx -\kappa\Delta$, and the situation is the same as for the Laplacian. On the other hand, when advection dominates, $\mathscr{L}\bar{u}^h \approx \boldsymbol{a} \cdot \nabla\bar{u}^h$, and $[\![b\bar{u}^h]\!] = [\![\kappa\, \partial\bar{u}^h/\partial n]\!]$ may be ignored. This time, the element residual, $\mathscr{L}\bar{u}^h$, is the source of error. A local distribution scheme would seem less than optimal because the Green's function propagates information along the integral curves of $-\boldsymbol{a}$ (keep in mind that the Green's function is for the adjoint operator, $\mathscr{L}^*$), with little amplitude decay. This means that there is an approximately constant trajectory of error corresponding to the residual error $\mathscr{L}\bar{u}^h$, in the element in question.

Finally, consider the Helmholtz operator, $\mathscr{L} = -\Delta - k^2$, $b = \partial/\partial n$, where k is the *wave number*. If k is real, we have *propagating waves*, whereas if k is imaginary, we have *evanescent* (decaying) *waves*. In the latter case, the Green's function is highly localized; as $|k| \to 0$ the Green's function approaches that for the Laplacian, as $|k| \to \infty$ the Green's function approaches $-k^{-2}\delta$, a delta function. In the case of propagating waves, the Green's function is oscillatory. In general, for $|k|$ large, the dominant source of error is the element residual, $\mathscr{L}\bar{u}^h = -k^2\bar{u}^h$. As $|k| \to 0$, the interface residual, $[\![b\bar{u}^h]\!] = [\![\partial\bar{u}^h/\partial n]\!]$, dominates.

4. Hierarchical *p*-refinement and bubbles

Hierarchical p-refinement plays an important role in clarifying the nature of the fine-scale Green's function, g', and provides a framework for its approximation. We begin by introducing some notations. Let

[1] This follows from the continuity of advective flux.

$$\bar{u}^h = \sum_{A=1}^{\bar{n}_{\text{nodes}}} \bar{N}_A \bar{u}_A \quad \text{(likewise } \bar{w}^h\text{)} \tag{46}$$

where $\bar{N}_A$ is a finite element shape function associated with the primary nodes, $A = 1, 2, \ldots, \bar{n}_{\text{nodes}}$, and $\bar{u}_A$ is the corresponding nodal values; and let

$$u' = \sum_{A=1}^{n'_{\text{nodes}}} N'_A u'_A \quad \text{(likewise } w'\text{)} \tag{47}$$

where N'_A is a hierarchical finite element shape function associated with the additional nodes, $A = 1, 2, \ldots, n'_{\text{nodes}}$, and u'_A are the corresponding hierarchical degrees of freedom. For example, let $\bar{u}^h$ be expanded in piecewise linear basis functions and u' in hierarchical cubics (see Fig. 9). Note, bubble functions are *zero* on element boundaries.

Substituting (46) and (47) into (17)–(20), and eliminating u'_A by *static condensation* results in

$$B(\bar{w}^h, \bar{u}^h; \tilde{g}') = L(\bar{w}^h; \tilde{g}') \quad \forall\, \bar{w}^h \in \bar{\mathcal{V}} \tag{48}$$

where

$$B(\bar{w}^h, \bar{u}^h; \tilde{g}') = a(\bar{w}^h, \bar{u}^h) + (\mathscr{L}^* \bar{w}^h, \tilde{M}'(\mathscr{L}\bar{u}^h)) \tag{49}$$

$$L(\bar{w}^h; \tilde{g}') = (\bar{w}^h, f) + (\mathscr{L}^* \bar{w}^h, \tilde{M}' f) \tag{50}$$

and

$$(\mathscr{L}^* \bar{w}^h, \tilde{M}'(\mathscr{L}\bar{u}^h)) = -\int_\Omega \int_\Omega (\mathscr{L}^* \bar{w}^h)(y) \tilde{g}'(x, y) (\mathscr{L}\bar{u}^h)(x)\, d\Omega_x\, d\Omega_y \tag{51}$$

$$\boxed{\tilde{g}'(x, y) = \sum_{A,B=1}^{n'_{\text{nodes}}} N'_A(y) [(\boldsymbol{K}'')^{-1}]_{AB} N'_B(x)} \tag{52}$$

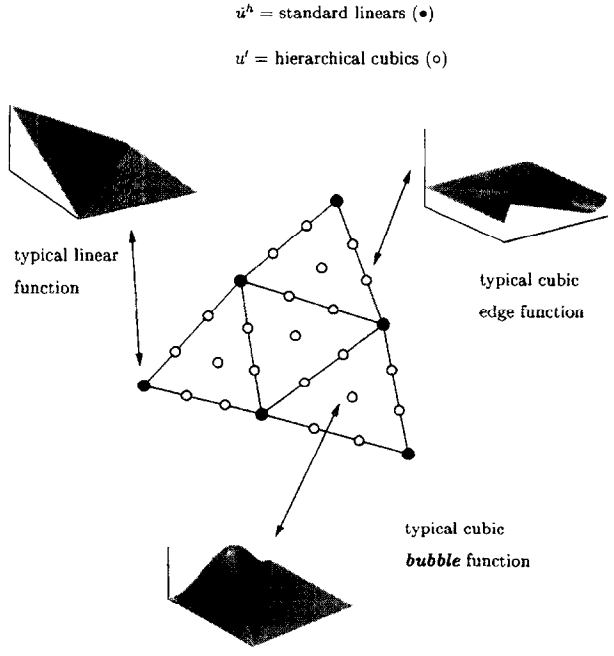

Fig. 9. Hierarchical cubics in two dimensions.

where

$$\boldsymbol{K}'' = [K''_{AB}] \tag{53}$$

$$K''_{AB} = a(N'_A, N'_B) \tag{54}$$

REMARKS

(1) Recall, $\mathscr{L}\bar{u}^h$ and $\mathscr{L}^*\bar{w}^h$ are *Dirac distributions* in the finite element case (cf. (51) and (39)).

(2) Hierarchical p-refinement generates an *approximate* fine-scale Green's function, $\tilde{g}' \approx g'$.

(3) For *implementational purposes*, it is more convenient to rewrite (49)–(51) in forms avoiding Dirac distributions. This can be accomplished by using the integration-by-parts formulas, viz.

$$(\mathscr{L}^*\bar{w}^h, \tilde{M}'(\mathscr{L}\bar{u}^h - f)) = \sum_{A,B=1}^{n'_{\text{nodes}}} a(\bar{w}^h, N'_A)[(\boldsymbol{K}'')^{-1}]_{AB}(a(N'_B, \bar{u}^h) - (N'_B, f)) \tag{55}$$

which amounts to the usual *static condensation* algorithm.

(4) A posteriori error estimation for the coarse-scale solution, $\bar{u}^h$, is provided by the fine-scale solution (see (38) and (44)):

$$\begin{aligned} u'(y) &= -\int_\Omega \tilde{g}(x, y)(\mathscr{L}\bar{u}^h - f)(x)\,d\Omega_x \\ &= -\int_{\Omega'} \tilde{g}'(x, y)(\mathscr{L}\bar{u}^h - f)(x)\,d\Omega_x - \int_{\Gamma'} \tilde{g}'(x, y)[\![b\bar{u}^h]\!](x)\,d\Gamma_x \\ &= -\sum_{e=1}^{n_{\text{el}}} \left(\int_{\Omega^e} \tilde{g}'(x, y)(\mathscr{L}\bar{u}^h - f)(x)\,d\Omega_x + \int_{\Gamma^e} \tilde{g}'(x, y)(b\bar{u}^h)(x)\,d\Gamma_x \right) \end{aligned} \tag{56}$$

or, in analogy with (55), by

$$u'(y) = -\sum_{A,B=1}^{n'_{\text{nodes}}} N'_A(y)[(\boldsymbol{K}'')^{-1}]_{AB}(a(N'_B, \bar{u}^h) - (N'_B, f)) \tag{57}$$

The quality of this estimator depends on the ability of $\{N'_A\}_{A=1}^{n'_{\text{nodes}}}$ to approximate the fine scales, or equivalently, the quality of the approximation $\tilde{g}' \approx g'$.

(5) Note that the fine-scale Green's function *only* depends on the hierarchical basis. The *exact* fine-scale Green's function corresponds to the limit $p \to \infty$.

(6) *The fine-scale Green's function is nonlocal*, but it is computed from a basis of functions having *compact support*. For example, in the two-dimensional case, the basis consists of bubbles, supported by individual elements, and edge functions, supported by pairs of elements sharing an edge. The three-dimensional case is similar, but somewhat more complicated; the basis consists of bubbles, face and edge functions. In three dimensions, pairs of elements support face functions whereas the number of elements supporting edge functions depends on the topology of the mesh.

(7) In two dimensions, by virtue of the convergence of hierarchical p-refinement, the exact fine-scale solution may be decomposed into a finite number of *limit functions*—one bubble for each element and one edge function for each pair of elements sharing an edge. In one dimension the situation is simpler in that only bubbles are required. The three-dimensional case is more complex in that bubbles, face and edge functions are required.

(8) Polynomial bubbles are typically ineffective, but so-called *residual-free bubbles* [2] are equivalent to exactly calculating element Green's functions. This approximation works exceptionally well in many important cases and will be discussed in more detail later on.

(9) If we consider *only* bubble functions in the refinement, coupling between different elements and all jump terms are *eliminated*. In this case,

$$(\mathscr{L}^*\bar{w}^h, \tilde{M}'(\mathscr{L}\bar{u}^h)) = -\int_{\Omega'}\int_{\Omega'} (\mathscr{L}^*\bar{w}^h)(y)\tilde{g}'(x, y)(\mathscr{L}\bar{u}^h)(x)\,d\Omega_x\,d\Omega_y \tag{58}$$

where Ω' has replaced Ω, and now the effect of u' is *nonlocal* only within each element. The approximate Green's function $\tilde{g}'$, is defined *element-wise* and takes on *zero* values on element boundaries.

5. Residual-free bubbles

The concept of *residual-free bubbles* has been developed and explored in [1–3,6–8,17,18]. The basic idea is to solve the fine-scale equation on individual elements with zero Dirichlet boundary conditions, viz. we wish to find $u' \in \mathcal{V}'$, such that $\forall \bar{u} \in \bar{\mathcal{V}}$,

$$\left.\begin{array}{ll} \Pi' \mathcal{L} u' = -\Pi'(\mathcal{L}\bar{u} - f) & \text{on } \Omega^e \\ u' = 0 & \text{on } \Gamma^e \end{array}\right\} \quad e = 1, 2, \ldots, n_{\text{el}} \tag{59}$$

Noting that $\bar{u}$ can be expressed in terms of the coarse-scale basis having support in the element in question, we realize that a fine-scale basis of residual-free bubbles can be constructed for each element, i.e.

$$\left.\begin{array}{ll} \Pi' \mathcal{L} N'_a = -\Pi'(\mathcal{L}\bar{N}_a - f) & \text{on } \Omega^e \\ N'_a = 0 & \text{on } \Gamma^e \end{array}\right\} \quad e = 1, 2, \ldots, n_{\text{el}} \tag{60}$$

where $a = 1, 2, \ldots, n_{\text{en}}$ is the local numbering of the primary nodes of element e. Thus, to each coarse-scale basis function $\bar{N}_a$, we solve (60) for a corresponding residual-free bubble N'_a. Consequently, the maximal dimension of the space of residual-free bubbles for element e is n_{en}. It is typical, however, that the dimension is less than n_{en}.

Brezzi and Russo [3] have constructed residual-free bubbles for the homogeneous advection–diffusion equation assuming the coarse-scale basis consists of continuous, piecewise linears on triangles. For this case $n_{\text{en}} = 3$, but the dimension of the space of residual-free bubbles is only one. Let B_e denote the residual-free bubble basis solution of the following problem:

$$\left.\begin{array}{ll} \mathcal{L} B_e = 1 & \text{on } \Omega^e \\ B_e = 0 & \text{on } \Gamma^e \end{array}\right\} \tag{61}$$

Note, due to the fact the coarse-scale space consist only of piecewise linears, combined with the fact that the fine-scale space satisfies zero Dirichlet boundary conditions, we can omit the projection operator, Π', present in the general case, namely (60), and solve (61) in the strong sense. However, in order to avoid potential linear dependencies, in general, we need to respect (60).

6. Element Green's functions

The idea of employing an *element Green's function* was proposed in our initial work on the variational multiscale method [10] (see also [13]). In place of (23)–(24), we solve the Green's function problem for each element:

$$\left.\begin{array}{ll} \Pi' \mathcal{L}^* g'_e(x, y) = \Pi' \delta(x - y) & \forall\, x \in \Omega^e \\ g'_e(x, y) = 0 & \forall\, x \in \Gamma^e \end{array}\right\} \quad e = 1, 2, \ldots, n_{\text{el}} \tag{62}$$

Use of element Green's functions in place of the global Green's function amounts to a *local approximation*,

$$\tilde{g}'(x, y) = g'_e(x, y) \quad \forall\, x, y \in \Omega^e, \qquad e = 1, 2, \ldots, n_{\text{el}} \tag{63}$$

The upshot is that the subgrid scales *vanish* on element boundaries, i.e.

$$u' = 0 \quad \text{on } \Gamma^e, \qquad e = 1, 2, \ldots, n_{\text{el}} \tag{64}$$

This means the subgrid scales are completely confined within element interiors.

There is an intimate link between element Green's functions and residual-free bubbles. This idea was first explored in [2], in which it was shown that, for the case governed by (61),

$$B_e(y) = \int_{\Omega^e} g'_e(x, y)\, d\Omega_x . \tag{65}$$

This result can be easily derived as follows:

$$\begin{aligned}\int_{\Omega^e} g'_e\, d\Omega &= (g'_e, 1)_{\Omega^e} \\ &= (g'_e, \mathscr{L}B_e)_{\Omega^e} \\ &= a(g'_e, B_e)_{\Omega^e} \\ &= (\mathscr{L}^* g'_e, B_e)_{\Omega^e} \\ &= (\delta, B_e)_{\Omega^e} \\ &= B_e\end{aligned} \tag{66}$$

Another way to derive (65) is to appeal to the general formula for the Green's function in terms of a fine-scale basis, namely (52). Specialized to the present case, (52) becomes

$$\tilde{g}'_e(x, y) = B_e(x)(a(B_e, B_e)_{\Omega^e})^{-1} B_e(y) \tag{67}$$

Note that

$$\begin{aligned}a(B_e, B_e)_{\Omega^e} &= (B_e, \mathscr{L}B_e)_{\Omega^e} \\ &= (B_e, 1)_{\Omega^e} \\ &= \int_{\Omega^e} B_e\, d\Omega\end{aligned} \tag{68}$$

By integrating (67) and using (68), we have

$$\begin{aligned}\int_{\Omega^e} \tilde{g}'_e(x, y)\, d\Omega_x &= \int_{\Omega^e} B_e(x)\, d\Omega_x (a(B_e, B_e)_{\Omega^e})^{-1} B_e(y) \\ &= B_e(y)\end{aligned} \tag{69}$$

REMARK. In general, the relationship between a fine-scale basis and a Green's function is given by (52). The result (65) is special to a residual-free bubble governed by (61).

7. Stabilized methods

Classical *stabilized methods* are generalized Galerkin methods of the form

$$a(\bar{w}^h, \bar{u}^h) + (\boldsymbol{L}\bar{w}^h, \tau(\mathscr{L}\bar{u}^h - f))_{\Omega'} = (\bar{w}^h, f) \tag{70}$$

where $\boldsymbol{L}$ is typically a *differential operator*, such as

$$\boldsymbol{L} = +\mathscr{L} \quad \text{Galerkin/least-squares (GLS)} \tag{71}$$

$$\boldsymbol{L} = +\mathscr{L}_{adv} \quad \text{SUPG} \tag{72}$$

$$\boldsymbol{L} = -\mathscr{L}^* \quad \text{Adjoint} \tag{73}$$

and τ is typically an *algebraic operator*. SUPG is a method defined for advective–diffusive operators, i.e. ones decomposable into advective ($\mathscr{L}_{\text{adv}}$) and diffusive ($\mathscr{L}_{\text{diff}}$) parts.

7.1. Relationship of stabilized methods with subgrid-scale models

It was shown in [10] that a stabilized method of *adjoint* type is an approximate subgrid-scale model in which the algebraic operator τ approximates the integral operator M' based on *element Green's functions*,

$$\tau = -\tilde{M}' \approx -M' \tag{74}$$

Equivalently,

$$\tau \cdot \delta(y-x) = \tilde{\mathrm{g}}'_e(x, y) \approx \mathrm{g}'(x, y) \tag{75}$$

Viz.

$$\begin{aligned}
&\int_{\Omega'}\int_{\Omega'} (-\mathscr{L}^*\overline{w}^h)(y)\tilde{\mathrm{g}}'_e(x, y)(\mathscr{L}\overline{u}^h - f)(x)\,\mathrm{d}\Omega_x\,\mathrm{d}\Omega_y \\
&\quad = \int_{\Omega'}\int_{\Omega'} (-\mathscr{L}^*\overline{w}^h)(y)\tau\cdot\delta(y-x)(\mathscr{L}\overline{u}^h - f)(x)\,\mathrm{d}\Omega_x\,\mathrm{d}\Omega_y \\
&\quad = \int_{\Omega'} (-\mathscr{L}^*\overline{w}^h)(x)\tau\cdot(\mathscr{L}\overline{u}^h - f)(x)\,\mathrm{d}\Omega_x
\end{aligned} \tag{76}$$

7.2. Formula for τ based on the element Green's function

The approximation

$$\tau\cdot\delta(y-x) \approx \mathrm{g}'_e(x, y) \tag{77}$$

suggests defining τ by

$$\int_{\Omega^e}\int_{\Omega^e} \tau\cdot\delta(y-x)\,\mathrm{d}\Omega_x\,\mathrm{d}\Omega_y = \int_{\Omega^e}\int_{\Omega^e} \mathrm{g}'_e(x, y)\,\mathrm{d}\Omega_x\,\mathrm{d}\Omega_y \tag{78}$$

$$\boxed{\tau = \frac{1}{\mathrm{meas}(\Omega^e)}\int_{\Omega^e}\int_{\Omega^e} \mathrm{g}'_e(x, y)\,\mathrm{d}\Omega_x\,\mathrm{d}\Omega_y} \tag{79}$$

REMARKS

(1) The element *mean value* of the Green's function provides the simplest definition of τ.

(2) This formula is adequate for low-order methods (h-adaptivity). For higher-order methods (p-adaptivity), accounting for variation of τ over an element may be required. In this case, we may assume for example that $\tau = \tau(x, y)$ is a polynomial of sufficiently high degree. Given an element Green's function g'_e we can in principle always calculate an equivalent function τ. Consequently, there is a *generalized stabilized method*, i.e. a method of the form,

$$a(\overline{w}^h, \overline{u}^h) - \sum_e \int_{\Omega^e}\int_{\Omega^e} \mathscr{L}^*\overline{w}^h(y)\tau(x, y)(\mathscr{L}\overline{u}^h - f)(x)\,\mathrm{d}\Omega_x\,\mathrm{d}\Omega_y = (\overline{w}^h, f) \tag{80}$$

equivalent to the element Green's function method. The generalized stabilized method involves determining τ such that the following *equivalence condition* is satisfied

$$\begin{aligned}
&\int_{\Omega^e}\int_{\Omega^e} \mathscr{L}^*\overline{w}^h(y)\tau(x, y)(\mathscr{L}\overline{u}^h - f)(x)\,\mathrm{d}\Omega_x\,\mathrm{d}\Omega_y \\
&\quad = \int_{\Omega^e}\int_{\Omega^e} \mathscr{L}^*\overline{w}^h(y)\mathrm{g}'_e(x, y)(\mathscr{L}\overline{u}^h - f)(x)\,\mathrm{d}\Omega_x\,\mathrm{d}\Omega_y \quad \forall\, \overline{w}^h, \overline{u}^h \in \overline{\mathscr{V}}
\end{aligned} \tag{81}$$

Thus, we have a full equivalence as indicated in Fig. 10. Examples of the calculation of τ by way of this procedure will be presented next.

EXAMPLES. We consider two one-dimensional examples, the advection–diffusion equation and the Helmholtz equation. In both cases we assume the use of standard piecewise linears for the coarse-scale basis. Consequently, determination of the element Green's function may be performed using the strong-form counterpart of (62), namely

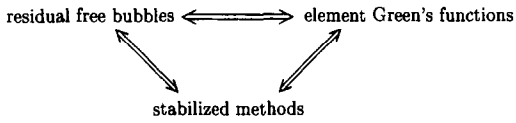

Fig. 10. Stabilized methods can be constructed which are equivalent to methods based on element Green's functions, which in turn are equivalent to methods developed from the residual-free bubbles concept. Historically, stabilized methods preceded the residual-free bubbles and element Green's function approaches, and there are certain stabilized methods (e.g. SUPG and GLS) which have been established for some time that are not, strictly speaking, equivalent to these concepts. Nevertheless, they have been justified independently by mathematical analysis and numerical testing.

$$\left.\begin{array}{ll} \mathscr{L}^* \mathrm{g}'_e(x, y) = \delta(x - y) & \forall\, x \in \Omega^e \\ \mathrm{g}'_e(x, y) = 0 & \forall\, x \in \Gamma^e \end{array}\right\} \quad e = 1, 2, \ldots, n_{\mathrm{el}} \tag{82}$$

REMARK. In *one dimension*, use of the element Green's function g'_e results in $u = \bar{u} + u'$ being *pointwise exact* for any

$$\bar{u} = \sum_{A=1}^{\bar{n}_{\mathrm{nodes}}} \bar{N}_A \bar{u}_A \tag{83}$$

and $\bar{u}$ being an end-node *interpolant* of u. This result holds for *all* problems.

7.2.1. Advection–diffusion equation ([10])

Let

$$\mathscr{L} = \mathscr{L}_{\mathrm{adv}} + \mathscr{L}_{\mathrm{diff}} \tag{84}$$

where

$$\mathscr{L}_{\mathrm{adv}} = a \frac{\mathrm{d}}{\mathrm{d}x} \tag{85}$$

$$\mathscr{L}_{\mathrm{diff}} = -\kappa \frac{\mathrm{d}^2}{\mathrm{d}x^2} \tag{86}$$

and a and κ are assumed to be positive constants. Consider the *homogeneous Dirichlet problem*

$$\mathscr{L}u = f \quad \text{in } \Omega = [0, L] \tag{87}$$

$$u = 0 \quad \text{on } \Gamma = \{0, L\} \tag{88}$$

Note that

$$\mathscr{L}^* = \mathscr{L}^*_{\mathrm{adv}} + \mathscr{L}^*_{\mathrm{diff}} \tag{89}$$

$$= -\mathscr{L}_{\mathrm{adv}} + \mathscr{L}_{\mathrm{diff}} \tag{90}$$

The solution of (82) is given by

$$\mathrm{g}'_e(x, y) = \begin{cases} C_1(y)(1 - \mathrm{e}^{-2\alpha x/h}) & x \leqslant y \\ C_2(y)(\mathrm{e}^{-2\alpha(x/h)} - \mathrm{e}^{-2\alpha}) & x \geqslant y \end{cases} \tag{91}$$

where

$$C_1(y) = \frac{1 - \mathrm{e}^{-2\alpha(1-(y/h))}}{a(1 - \mathrm{e}^{-2\alpha})} \tag{92}$$

$$C_2(y) = \frac{\mathrm{e}^{2\alpha(y/h)} - 1}{a(1 - \mathrm{e}^{-2\alpha})} \tag{93}$$

$$\alpha = \frac{ah}{2\kappa} \quad \text{(element Péclet number)} \tag{94}$$

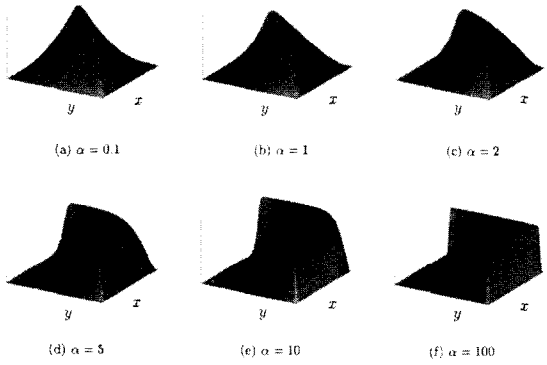

Fig. 11. Element Green's function for the one-dimensional advection–diffusion equation as a function of element Péclet number (α).

and $h = \text{meas}(\Omega^e)$ is the element length. This element Green's function is shown in Fig. 11 for various element Péclet numbers.

By virtue of the fact that the coarse scales are piecewise linear and $\mathscr{L}\bar{u}^h$ and $\mathscr{L}^*\bar{w}^h$ are therefore constants on each element, the simple formula (79) suffices to define a constant τ satisfying (81), that is, one equivalent to use of the element Green's function, viz.

$$\begin{aligned}\tau &= \frac{1}{\text{meas}(\Omega^e)} \int_{\Omega^e} \int_{\Omega^e} \mathrm{g}'_e(x, y)\, \mathrm{d}\Omega_x\, \mathrm{d}\Omega_y \\ &= \frac{h}{2a}\left(\coth \alpha - \frac{1}{\alpha}\right)\end{aligned} \tag{95}$$

REMARKS

(1) This is a well-known formula from the theory of stabilized methods.
(2) This τ results in a *nodally exact* stabilized method for piecewise linear $\bar{N}_A$'s and constant f. Remarkably, element lengths need *not* be uniform.
(3) The approximate fine scale solution is given by

$$u'(y) \approx -\int_{\Omega'} \tilde{\mathrm{g}}'(x, y)(\mathscr{L}\bar{u}^h - f)(x)\, \mathrm{d}\Omega_x - \int_{\Gamma'} \tilde{\mathrm{g}}'(x, y)[\![b\bar{u}^h]\!](x)\, \mathrm{d}\Gamma_x \tag{96}$$

For the advection-dominated case we can neglect the jump term and make use of the approximation $\mathscr{L}\bar{u}^h \approx \boldsymbol{a}\cdot\nabla\bar{u}^h$. Further, employing the approximation (75), we have

$$u' \approx -\tau(\boldsymbol{a}\cdot\nabla\bar{u}^h - f) \tag{97}$$

Assuming τ has the form $h/(2|\boldsymbol{a}|)$ in the advection-dominated case, (97) becomes

$$u' \approx -\frac{h}{2|\boldsymbol{a}|}(\boldsymbol{a}\cdot\nabla\bar{u}^h - f) \tag{98}$$

This may be used as a simple, local error estimator for the advection-dominated case.

7.2.2. *Helmholtz equation (Oberai-Pinsky [16])*

The set-up is identical to the previous example. We consider the Dirichlet problem (87)–(88), for the Helmholtz equation in which

$$\mathscr{L} = -\frac{\mathrm{d}^2}{\mathrm{d}x^2} - k^2 \tag{99}$$

is the Helmholtz operator and k is the *wave number*. We assume $k \in \mathbb{R}$, corresponding to the case of *propagating waves*. Note $\mathscr{L}^* = \mathscr{L}$. The Green's function for an element of length h is given by

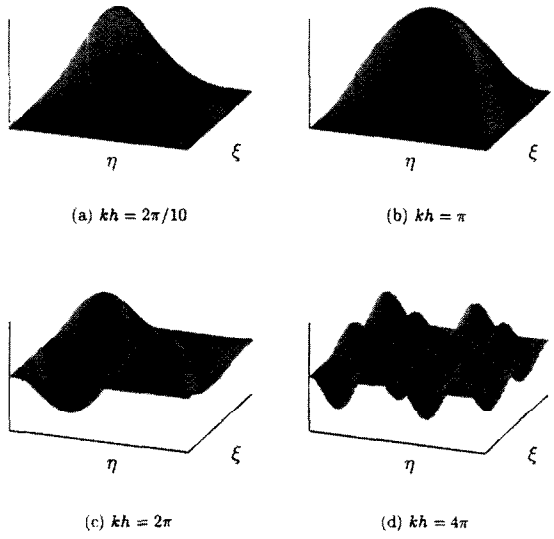

Fig. 12. Element Green's function (kg'_e) for the one-dimensional Helmholtz equation as a function of element wave number (kh).

$$g'_e(\xi,\eta)=\begin{cases}\dfrac{\sin(kh(1+\xi)/2)\sin(kh(1-\eta)/2)}{k\sin(kh)}, & \xi<\eta\\ \dfrac{\sin(kh(1-\xi)/2)\sin(kh(1+\eta)/2)}{k\sin(kh)}, & \xi\geqslant\eta\end{cases} \tag{100}$$

where ξ and η are normalized, bi-unit coordinates,

$$-1\leqslant\xi,\eta\leqslant+1 \tag{101}$$

The element Green's function is depicted in Fig. 12 for various *element wave numbers*.

This time $\mathscr{L}\bar{u}^h$ and $\mathscr{L}^*\bar{w}^h$ vary linearly over each element and satisfaction of the equivalence condition, (81), entails a non-constant τ, as follows:

$$\tau(\xi,\eta)=\tau_{00}+\tau_{11}\xi\eta\approx g'_e(\xi,\eta) \tag{102}$$

where

$$\tau_{ij}=\frac{\displaystyle\int_{-1}^{+1}\int_{-1}^{+1}\xi^i\eta^j g'_e(\xi,\eta)\,d\xi\,d\eta}{\displaystyle\int_{-1}^{+1}\int_{-1}^{+1}\xi^{2i}\eta^{2j}\,d\xi\,d\eta} \tag{103}$$

REMARKS

(1) Oberai and Pinsky [16] have also derived an element Green's function in two dimensions for a bilinear rectangle and an equivalent τ. Similar results for three dimensions are also easily derived.

(2) As in the previous example, this τ results in a *nodally exact* stabilized method for piecewise linear $\bar{N}_A$'s and constant f, for an arbitrary non-uniform mesh.

8. Beyond residual-free bubbles

The residual-free bubbles concept is established by way of its equivalence with mathematically proven stabilized methods. To make further improvement, we need to acknowledge the presence of functions other than bubbles. As discussed in Section 4, bubbles and edge functions can be constructed in two dimensions in such a way as to decompose the exact fine-scale solution in terms of functions with local support. To determine the

exact basis of bubbles and edge functions is problematic due to the fact that they do not have disjoint support. Consequently, uncoupled, local evaluation is not feasible and the coupled analytical problem appears virtually impossible to solve. However, it would seem that improvement, beyond that achieved with bubbles alone, could be attained by adding some kind of edge functions to the formulation to reduce the distributional component of error concentrated on element interfaces. This leads us to consider approximate problems governing residual-free functions in which simplifications have been introduced ab initio to avoid coupling.

As an example, consider the set-up for two contiguous linear triangular elements illustrated in Fig. 13. The idea is to define residual-free edge functions on pairs of elements ignoring the coupling introduced by edge functions associated with overlapping pairs of elements. Intuitively, functions defined in this way would appear beneficial but, of course, not capable of removing the distributional part of error entirely. For each pair of contiguous elements, the following problem is to be solved: Find $N'_A \in \mathscr{V}'(\omega)$, $A = 1, 2, 3, 4$, such that $\forall\, v' \in \mathscr{V}'(\omega)$,

$$\begin{aligned}(v', \mathscr{L}N'_A)_\omega &= -(v', \mathscr{L}(\overline{N}_A + B_A^- + B_A^+) - f)_\omega \\ &= -(v', \mathscr{L}(\overline{N}_A + B_A^- + B_A^+) - f)_{\omega^-} - (v', [\![b(\overline{N}_A + B_A^- + B_A^+)]\!])_{\gamma'}\end{aligned} \tag{104}$$

where N'_A is a residual-free edge function, B_A^- and B_A^+ are bubbles with support in Ω^- and Ω^+, respectively, and

$$\mathscr{V}'(\omega) = \{v \in H^1(\omega) | v = 0 \quad \text{on } \gamma\} \tag{105}$$

(Due to possible linear dependencies, the number of independent bubbles and edge functions may be reduced.) To make things a bit more specific, we can select bubbles to remove residuals on element interiors, as follows:

$$(v', \mathscr{L}B_{a^-}^-)_{\Omega^-} = -(v', \mathscr{L}\overline{N}_{a^-} - f)_{\Omega^-} \quad \forall\, v' \in \mathscr{V}^1(\Omega^-), \quad a^- = 1, 2, 3 \tag{106}$$

$$(v', \mathscr{L}B_{a^+}^+)_{\Omega^+} = -(v', \mathscr{L}\overline{N}_{a^+} - f)_{\Omega^+} \quad \forall\, v' \in \mathscr{V}^1(\Omega^+), \quad a^+ = 1, 2, 3 \tag{107}$$

where

$$\mathscr{V}'(\Omega^-) = \{v \in H^1(\Omega^-) | v = 0 \quad \text{on } \Gamma^-\} \tag{108}$$

$$\mathscr{V}'(\Omega^+) = \{v \in H^1(\Omega^+) | v = 0 \quad \text{on } \Gamma^+\} \tag{109}$$

Then, the edge functions need to satisfy

$$(v', \mathscr{L}N'_A)_\omega = -(v', [\![b(\overline{N}_A + B_A^- + B_A^+)]\!])_{\gamma'} \quad \forall v' \in \mathscr{V}'(\omega), \quad A = 1, 2, 3, 4 \tag{110}$$

Note that, in this case, $\mathscr{L}N'_A = 0$ on ω', but N'_A is nontrivial due to the jump term on γ' which acts as a source.

Further simplifications may be envisioned. For example, one could ignore the distributional contribution of the bubbles in (104), and define the edge functions by

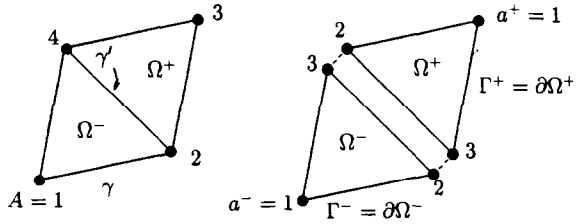

$$\omega' = \Omega^- \cup \Omega^+$$
$$\omega = \overline{\omega'}$$
$$\gamma' = \Gamma^- \cap \Gamma^+$$
$$\gamma = (\Gamma^- \cup \Gamma^+) \backslash \gamma'$$

Fig. 13. Typical patch of two contiguous linear triangles.

$$(v', \mathscr{L}N'_A)_\omega = -(v', [\![b\bar{N}_A]\!])_\gamma, \quad \forall v' \in \mathscr{V}'(\omega), \quad A = 1, 2, 3, 4 \tag{111}$$

Various other possibilities suggest themselves. We hope to pursue this topic by way of specific examples in future work.

REMARK. These ideas are related to recent work of Franca and Russo [5] in which the residual-free condition is satisfied on macroelements.

9. Summary

We have given a general variational multiscale formulation of an abstract Dirichlet problem. We considered the case in which finite elements are used to represent the coarse scales and we derived an exact equation governing the coarse scales. This equation amounts to the Galerkin formulation plus an additional term which depends on the distributional form of the residual (i.e. element interior and interface jump terms) and a fine-scale Green's function. A representation is also derived for the fine-scale solution, which amounts to the error in the coarse scales. The results serve as paradigms for subgrid-scale models and a posteriori error estimators.

To understand the nature of the fine-scale Green's function, we considered hierarchical p-refinement and bubbles. An explicit formula for the fine-scale Green's function is obtained in terms of the hierarchical (i.e. fine scale) basis. This formula suggests that the fine-scale Green's function can be represented in terms of a basis of functions having local support. Subsequent discussion dealt with developing practical approximations.

We reviewed the concepts of residual-free bubbles, element Green's functions, and stabilized methods, and summarized the relationships between them.

We also presented some initiatory ideas on developing better-quality, approximate, residual-free bases by including edge functions in addition to bubbles in two dimensions, etc.

We believe the variational multiscale method has considerable potential for important classes of problems in science and engineering. The major obstacles to be faced are explicit, analytic development of better quality, residual-free bases for problems of practical interest. Various ideas are being pursued at this time to address these issues.

Acknowledgements

Brazilians and Italians are almost as good at soccer as they are at mathematics. We acknowledge the inspirations provided by our collaborators Franco Brezzi, Leo Franca and Alessandro Russo. This research was supported by the Office of Naval Research under Grant N00014-96-1-0109.

References

[1] C. Baiocchi, F. Brezzi and L.P. Franca, Virtual bubbles and the Galerkin/least-squares method, Comput. Methods in Appl. Mech. and Engrg. 105: (1993) 125–142.
[2] F. Brezzi, L.P. Franca, T.J.R. Hughes and A. Russo, $b = \int g$, Comput. Methods in Appl. Mech. and Engrg. 145 (1997) 329–339.
[3] F. Brezzi and A. Russo, Choosing bubbles for advection–diffusion problems, Math. Models Methods Appl. Sci. (1994) 571–587.
[4] J. Douglas Jr. and J.P. Wang, An absolutely stabilized finite element method for the Stokes problem, Math. Comput. 52 (1989) 495–508.
[5] L.P. Franca and A. Russo, Approximation of the Stokes problem by residual-free macro bubbles, East–West J. Numer. Anal. 4 (1996) 265–278.
[6] L.P. Franca and A. Russo, Deriving upwinding, mass lumping and selective reduced integration by residual-free bubbles, Appl. Math. Lett. 9 (1996) 83–88.
[7] L.P. Franca and A. Russo, Mass lumping emanating from residual-free bubbles, Comput. Methods Appl. Mech. Engrg. 142 (1997) 353–360.
[8] L.P. Franca and A. Russo, Unlocking with residual-free bubbles, Comput. Methods in Appl. Mech. Engrg. 142 (1997) 361–364.

[9] L.P. Franca, T.J.R. Hughes and R. Stenberg, Stabilized finite element methods for the Stokes problem, In: M.D. Gunzburger and R.A. Nicolaides, eds., Incompressible Computational fluid dynamics (Cambridge University Press, Cambridge, 1993) 87–107.
[10] T.J.R. Hughes, Multiscale phonomena: Green's functions, the Dirichlet-to-Neumann formulation, subgrid scale models, bubbles and the origins of stabilized methods, Comput. Methods Appl. Mech. Engrg. 127 (1995) 387–401.
[11] T.J.R. Hughes and L.P. Franca, A new finite element formulation for computational fluid dynamics. VII. The Stokes problem with various well-posed boundary conditions: Symmetric formulations that converge for all velocity/pressure spaces, Comput. Methods Appl. Mech. Engrg. 65 (1987) 85–96.
[12] T.J.R. Hughes and G.M. Hulbert, Space–time finite element methods for elastodynamics: Formulations and error estimates, Comput. Methods Appl. Mech. Engrg. 66 (1988) 339–363.
[13] T.J.R. Hughes and J. Stewart, A space–time formulation for multiscale phenomena, J. Comput. Appl. Math. 74 (1996) 217–229.
[14] G.M. Hulbert and T.J.R. Hughes, Space–time finite element methods for second-order hyperbolic equations, Comput. Methods Appl. Mech. Engrg. 84 (1990) 327–348.
[15] K. Jansen, C. Whiting, S. Collis and F. Shakib, A better consistency for low-order stabilized finite-element methods, Preprint, 1997.
[16] A.A. Oberai and P.M. Pinsky, A multiscale finite element method for the Helmholtz equation, Comput. Methods Appl. Mech. Engrg. 154 (1998) 281–297.
[17] A. Russo, Bubble stabilization of finite element methods for the linearized incompressible Navier–Stokes equations, Comput. Methods Appl. Mech. Engrg. 132 (1996) 335–343.
[18] A. Russo, A posteriori error estimators via bubble functions, Math. Models Methods Appl. Sci., 6 (1996) 33–41.